[18] S. S. Kim, W. Zhang, T. J. Pinnavaia, *Science* **1998**, *282*, 1302.
[19] Y. Shin, J. Liu, J. H. Chang, Z. Nie, G. J. Exarhos, *Adv. Mater.* **2001**, *13*, 728.
[20] M. Wu, X.-Y. Liu, C. S. Strom, P. Bennema, W. van Enckevort, N.-B. Ming, *Phys. Rev. Lett.* **1998**, *80*, 3089.
[21] S. Busch, H. Dolhaine, A. DuChesne, S. Heinz, O. Hochrein, F. Laeri, O. Podebrad, U. Vietze, T. Weiland, R. Kniep, *Eur. J. Inorg. Chem.* **1999**, 1643.
[22] C. S. Strom, P. F. P. Grimbergen, P. Bennema, H. Meekes, M. A. Verheijen, L. J. P. Vogels, M. Wang in *Molecular Modeling Applications in Crystallization* (Ed.: A. S. Myerson), Cambridge University Press, Cambridge, **1999**, pp. 228–312.
[23] C. T. Kresge, M. E. Leonowicz, W. J. Roth, J. C. Vartuli, J. S. Beck, *Nature* **1992**, *359*, 710.
[24] J. S. Beck, J. C. Vartuli, W. J. Roth, M. E. Leonowicz, C. T. Kresge, K. D. Schmitt, C. T.-W. Chu, D. H. Olson, E. W. Sheppard, S. B. McCullen, J. B. Higgins, J. L. Schlenker, *J. Am. Chem. Soc.* **1992**, *114*, 10834.
[25] S. Inagaki, S. Guan, Y. Fukushima, T. Ohsuna, O. Terasaki, *J. Am. Chem. Soc.* **1999**, *121*, 9611.
[26] M. H. Lim, A. Stein, *Chem. Mater.* **1999**, *11*, 3285.
[27] T. Asefa, M. J. MacLachlan, N. Coombs, G. A. Ozin, *Nature* **1999**, *402*, 867.
[28] Many papers have been published in this area by many groups, which include those of Professors Ozin, Stein, Sayari, Inagaki. A complete list of publications is beyond the purpose of this paper, but Professor Stein published a good review article: A. Stein, B. J. Melde, R. C. Schroden, *Adv. Mater.* **2000**, *12*, 1403.
[29] O. Dag, C. Yoshina-Ishii, T. Asefa, M. J. MacLachlan, H. Grondey, N. Coombs, G. A. Ozin, *Adv. Funct. Mater.* **2001**, *11*, 213.
[30] H. Y. Fan, S. Reed, T. Baer, R. Schunk, G. P. Lopez, C. J. Brinker, *Microporous Mesoporous Mater.* **2001**, *44*, 625.
[31] S. Guan, S. Inagaki, T. Ohsuna, O. Terasaki, *J. Am. Chem. Soc.* **2000**, *122*, 5660.
[32] B. C. Bunker, P. C. Rieke, B. J. Tarasevich, A. A. Campbell, G. E. Fryxell, G. L. Graff, S. Song, J. Liu, J. W. Virden, *Science* **1994**, *264*, 48.
[33] Other curved morphologies such as discoids, doughnuts, and cupcakes were also observed at a lower surfactant concentration. The curved geometry is consistent with the curved shapes reported in hexagonal mesophase materials and will not be discussed here.
[34] A. F. Wells, *Structural Inorganic Chemistry Clarendon Press*, 5th ed., Oxford University Press, Oxford, **1984**.

Metalloprotein Conformation

Sliding Helix and Change of Coordination Geometry in a Model Di-Mn^{II} Protein**

William F. DeGrado, Luigi Di Costanzo, Silvano Geremia, Angela Lombardi, Vincenzo Pavone, and Lucio Randaccio*

In metalloenzymes, the protein matrix tunes the dynamic and structural properties of their metal ion cofactors to catalyze a wide range of reactions with remarkable catalytic efficiencies.[1] As the reaction proceeds, the metal ions must cycle between different ligation and sometimes also oxidation states;[2] the protein plays an active role in stabilizing and catalyzing the interconversion of these intermediates.[3–5] Shifts of key carboxylate side chains and other localized motions are often observed in response to changes in oxidation state and the binding of exogenous ligands.[6–8] The de novo design of novel artificial proteins that have predictable structures and functions is the most challenging goal in protein design and mimicry. Creating functional artificial metalloproteins requires a detailed understanding of the protein-folding mechanism as well as of the coordination chemistry of the metal centers. Herein we demonstrate a sliding-helix mechanism for stabilizing a change in the ligand environment of DF1, a model di-Mn^{II} protein.

Recently, we designed DF1 as a highly simplified model for diiron/dimanganese proteins.[9] This class of protein includes a number of functionally diverse structures including diiron proteins such as the radical-forming R2 subunit of ribonucleotide reductase[10] and methane monooxygenase,[11] as well as dimanganese proteins[12] such as catalase[13] and arginase.[14] DF1 is a dimer of helix-loop-helix motifs with a dimetal site near the center of the four-helix-bundle structure. As in natural diiron proteins, two Glu side chains bridge both metal ions, while the other two carboxylates interact with a

[*] Prof. S. Geremia, Dr. L. Di Costanzo, Prof. L. Randaccio
Center of Excellence in Biocrystallography
Department of Chemical Sciences, University of Trieste
Via L. Giorgieri 1, 34127 Trieste (Italy)
Fax: (+39) 040-558-3903
E-mail: geremia@univ.trieste.it
Prof. W. F. DeGrado
Department of Biochemistry and Biophysics
School of Medicine, University of Pennsylvania
Philadelphia, PA 19104-6059A (USA)
Prof. A. Lombardi, Prof. V. Pavone
Department of Chemistry, University of Naples "Federico II"
Complesso Universitario Monte S'Angelo
Via Cynthia 45, 80126 Naples (Italy)

[**] This work was supported by the MIUR (PRIN MM03185591), NIH grant GM54616, and by the MRSEC program of the NSF (award DMR0079909. We thank Ben North for many helpful discussions and preliminary calculations.

Supporting information for this article is available on the WWW under http://www.angewandte.org or from the author.

single metal ion in a bidentate, chelating interaction. Two His residues form additional monodentate ligands. The minimalist design of DF1 renders it an excellent candidate for determining how the tertiary and quaternary structures respond to changes in the ligation of dimetal centers. Direct access to the dimetal site of DF1 is controlled by the nature of the side chain at positions 13 and 13′ of equivalent monomers; with Leu at these positions, the protein binds two Co^{II}, Zn^{II}, or Mn^{II} ions without exogenous ligands.[9] Reducing the bulk of residue 13 and 13′ to Ala allows access of small molecules to the active site, and the X-ray structure of the di-Mn^{II} revealed a bridging DMSO group, whose sulfoxide oxygen atom is in direct contact with both manganous ions.[15] Herein we report the crystal structure of DF1–L13G–DF1, in which the active-site cavity has been expanded by further reducing the bulk of residue 13 to Gly.

The structure of di-Mn^{II}–L13G–DF1 displays four crystallographically independent dimers in the asymmetric unit. The individual dimers are closely related to the structure of di-Mn^{II}–L13A–DF1, with the exception that the water-filled access channel has been expanded in the expected manner. The most striking feature found in di-Mn^{II}–L13G–DF1 is the presence of two different dimanganese coordination environments. In three of the four dimers (AB, CD, and EF) a solvent molecule bridges the two metal ions (Figure 1a), while in the fourth dimer (GH) two terminal solvent molecules are coordinated to the two manganese ions *trans* to the histidine ligands (Figure 1b). The electron density of the four dimetal centers is well-defined, and there is no evidence for a mixture of binding modes within a given active site. Dimanganous derivatives of analogues of DF1 are very resistant to air oxidation in solution (unpublished data), and the observed coordination geometries observed in the crystal structure are consistent with the Mn^{II} oxidation state.

The bridging solvent molecules in AB, CD, and EF have been tentatively assigned as water molecules, based on the Mn–Mn and Mn–O distances, and in view of the pH value at which the crystals were grown.[16] The solvent-bridged centers show an intermetal distance of 3.59 Å (mean value), which is close to the value of 3.61 Å observed in small-molecule complexes for water-bridged di-Mn^{II} centers that are also bridged by two 1,3-carboxylate groups.[17] A significantly shorter distance would be expected for higher oxidation states of Mn ions in the presence of bridging exogenous anions.[13] In di-Mn^{II}–L13G–DF1 the Mn–O distances of the bridging solvent ligand range from 2.3 to 2.5 Å, which is somewhat larger than the 2.2-Å distance generally observed in analogous small-molecule H_2O–Mn^{II}_2 complexes.[17–19] In the GH dimer with two terminal solvent molecules, the intermetal distance increases to 4.20 Å. The two axial Mn–solvent

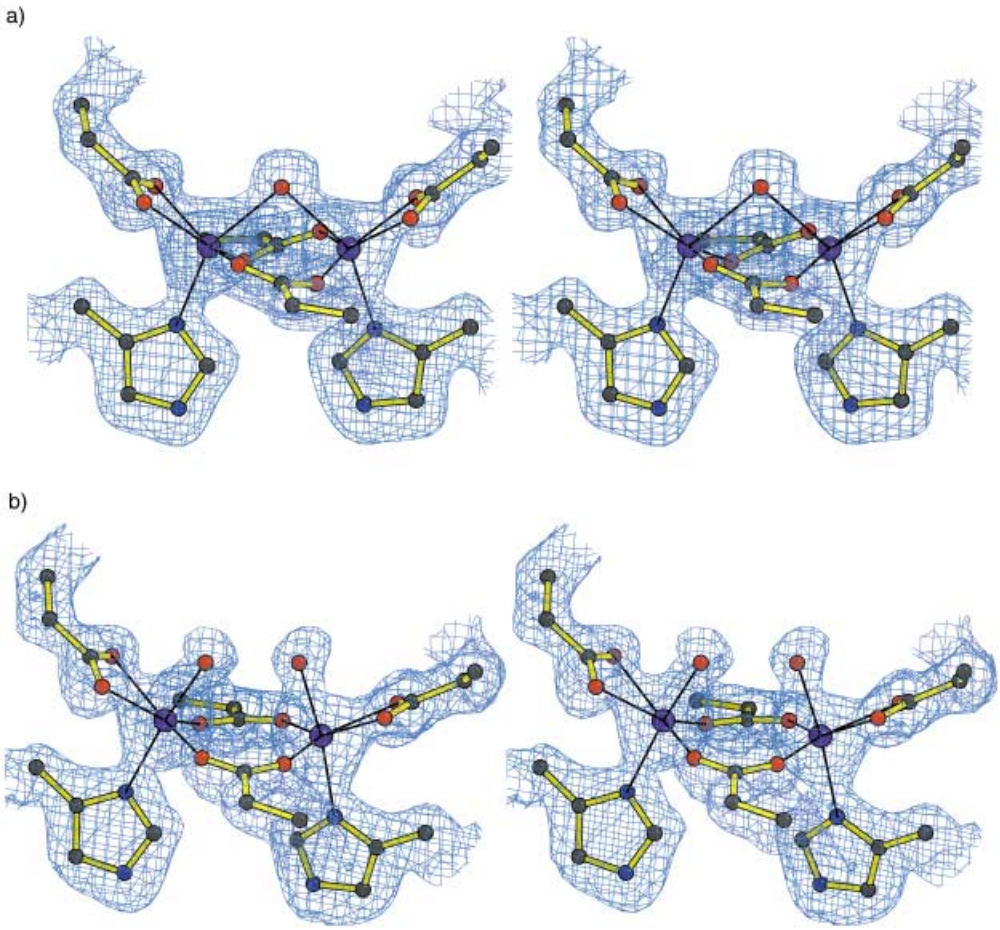

Figure 1. Stereoview of 2*Fo-Fc* electron-density maps (contour levels are 1.5σ) of the dinuclear metal-binding site of di-Mn–L13G–DF1 in the AB dimer (a) and in the GH dimer (b). These figures were generated with Bobscript.[29]

  0044-8249/03/11504-0434 $ 20.00+.50/0

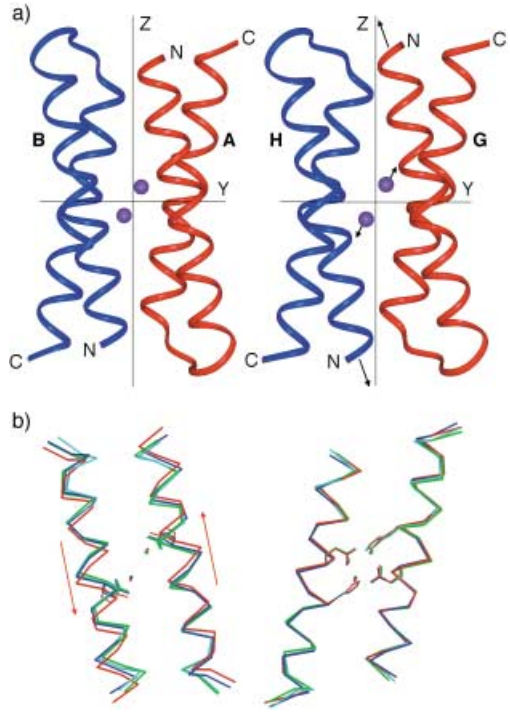

Figure 2. a) Crystallographically independent dimers of di-Mn–L13G–DF1, AB (left) and GH (right), viewed along the x axis of a common orthogonal reference system. The arrows in the GH dimer indicate the shifts of N-terminal helices and metal ions with respect to the other dimers. This figure was generated with InsightII (BIOSYM, San Diego, CA). b) Superimposition of helices 1 and 1′ (left) and helices 2 and 2′ (right) of the four crystallographically independent dimers of di-Mn^{II}–L13G–DF1. Note the movement of helices 1 and 1′ of the GH pair (red) relative to the remaining helices (AB blue; CD green; EF cyan). The Figure was generated with Rasmol.[30]

distances are 2.0 and 2.1 Å, which are significantly shorter than the corresponding distances found in simpler dinuclear manganese aqua complexes (ca. 2.3 Å).[20,21] We also observe a close approach of the two terminal solvent molecules (2.7 Å), which suggests that the pair of solvent molecules might actually be a more tightly chelated $H_3O_2^-$.[6]

To investigate the structural consequences of the different modes of binding, we analyzed crystal packing, local shifts in side-chain conformations, as well as global shifts in tertiary structure. The analysis of the differences in crystal-lattice packing among the four-helix bundles (see Supporting Information) revealed no significant relationship between the packing environment and the different structural behavior of these molecules. In GH, the carboxylate planes are rotated with respect to each other by an angle of 20°; in the other dimers small changes in the Glu side-chain torsions result in more acute carboxylate plane angles ranging from 32 to 40°. A more deep-seated change in quaternary structure was discovered when the bundles were examined in a common Cartesian coordinate system in which the central axis of the bundle is aligned along the z axis and the approximate C_2 axis of symmetry of the metal-binding site is aligned along the x axis (Figure 2). The C-terminal helices (2 and 2′), which contain the His-Xxx-Xxx-Glu liganding site, are virtually invariant among the structures (Table 1 and Figure 2). In contrast, the N-terminal helices (1 and 1′), each of which contains only a single liganding Glu side chain, occupy different positions in the GH dimer relative to the other structures. In GH the two copies of helix 1 undergo a shift in opposite directions (approximately 0.7 Å) along the Z axis, away from the metal-binding site (Table 1 and Figure 2). Indeed, this shift accompanies the lengthening of the metal–metal distance observed in the GH dimer.

In summary, this analysis has revealed a novel, sliding-helix mechanism by which metalloproteins can accommodate changes in their coordination environment. Although similar mechanisms have been shown to be important for signal transduction,[22,23] such motions have not been observed in the dimetal class of metalloenzymes. Instead, previous studies of catalytically active metalloproteins have focused on more localized carboxylate shifts and changes to isolated regions of the backbone.[6] Indeed, the idealized structure of DF1 has facilitated this analysis, which might have been more difficult to observe in a complex, large protein. Our data show that more collective motions provide an attractive mechanism for dynamic conformational tuning in designed metalloproteins. It will be interesting to determine whether this mechanism contributes to the catalytic activities of natural metalloproteins as well.

Table 1: Angles formed by each axis of helices for the four dimers of Mn^{II}–L13G–DF1 with the axes of the reference system, together with the coordinates of the center of mass of the individual helices. The only significant deviation between the equivalent helices of GH relative to the other dimers lies within helix 1 of G and H (bold values).

Helix	Angles			Centre of mass		
	x [°]	*y* [°]	*z* [°]	*x* [Å]	*y*[Å]	*z*[Å]
HEL 1-A	−97	−78	−166	4.52	5.41	0.13
HEL 1-C	−102	−78	−163	4.52	5.07	−0.13
HEL 1-E	−102	−78	−163	4.59	5.14	−0.07
HEL 1-G	−97	−77	−165	4.62	5.32	**0.68**
HEL 1′-B	99	102	15	4.53	−5.38	−0.03
HEL 1′-D	101	104	18	4.33	−5.16	0.17
HEL 1′-F	99	101	14	4.35	−5.16	0.15
HEL 1′-H	97	103	14	4.56	−5.40	**−0.78**
HEL 2-A	82	78	−15	−4.55	5.85	2.08
HEL 2-C	76	76	−20	−4.40	5.95	1.93
HEL 2-E	77	78	−18	−4.47	5.89	2.06
HEL 2-G	81	77	−16	−4.51	6.00	2.12
HEL 2′-B	−80	−102	164	−4.45	−5.91	−2.18
HEL 2′-D	−79	−102	163	−4.48	−5.81	−1.91
HEL 2′-F	−80	−101	165	−4.65	−5.85	−2.10
HEL 2′-H	−82	−103	164	−4.59	−5.93	−2.03

  0044-8249/03/11504-0435 $ 20.00+.50/0

Experimental Section

Crystallization and data collection: Single crystals of the complex di-Mn^{II}–L13G–DF1 were grown at 277 K using the hanging-drop vapor-diffusion method. The protein was solubilized as described previously,[15] and drops were prepared by adding 2 μL of protein (10 mg mL^{-1}) to 2 μL of reservoir solution containing PEG 400 (34%), $Mn(CH_3COO)_2$ (0.03 M), Tris–HCl (0.1 M of pH 7.5). Diamond-shaped crystals of di-Mn^{II}–L13G–DF1 ($0.3 \times 0.3 \times 0.2$ mm^3) grew within 10 days at 277 K. X-ray diffraction data were collected at the Elettra Synchrotron (Trieste, Italy) using a monochromatic radiation ($\lambda =$ 1.200 Å) and a MAR Research 345-mm imaging plate as detector. The crystal used in the collection data was harvested into mother liquor with a small loop of fine rayon fiber and flash-frozen in a stream of N_2 at 100 K. The data were collected at a resolution of 1.91 Å, fixing the crystal–detector distance at 180 cm. The crystal belongs to the space group $P2_12_12_1$ with unit-cell parameters of $a =$ 38.22, $b = 89.27$, $c = 146.29$ Å. The determination of unit-cell parameters, integration of reflection intensities, and data scaling were performed using MOSFLM and SCALA from the CCP4 program suite.[24] The data set consists of 94932 measured reflections and provides a unique data set of 38634 reflections with an $R_{merge} = 0.125$ and an overall completeness to 1.91 Å of 0.966. R_{merge} in the 2.01–1.91 resolution shell is 0.463.

Structure determination: the V_M values suggested the presence of 32 or 40 monomer chains in the unit cell and 8 or 10 monomers in the asymmetric unit. The structure of the complex di-Mn–L13G–DF1 was solved by molecular replacement with the program AMORE[25] using the coordinates of one dimer of the crystal structure of di-Mn^{II}–L13A–DF1[15] as the starting model. Four rotation/translation solutions were found for the independent dimers, compatible with the complete crystal packing. The first rigid body refinement of the four dimers gave an R factor of 0.420. The structure was refined with the REFMAC program[26] using 36674 unique reflections following a process of manual model building by using the program O[27] (5% of the data set was selected for the calculation of the R_{free}). The final R factor was 0.201 and $R_{free} = 0.244$.

Structure analysis: each four-helix bundle was positioned in a common orthogonal coordinate system using the following algorithm: 1) The regression line passing through the midpoints of pseudoequivalent C_α pairs of the N-terminal helices (residues 1–22) and of C-terminal helices (residues 27–48) defines the direction of the x axis, which coincides with the approximate, noncrystallographic twofold axis of the dimer. 2) The regression line passing through the midpoints of pseudoequivalent C_α pairs of diagonally opposing helices (the N-terminal helix of one monomer with the C-terminal helix of the other monomer) projected on the plane orthogonal to the x direction defines the z axis, which coincides with the super-helix axis. 3) The equation of the best line passing through the point of origin[28] of one helix in this reference system describes the position of the single helices (Table 1). Crystallographic data have been deposited in the Protein Data Bank, access number 1 LT1.

Received: May 29, 2002
Revised: October 11, 2002 [Z19403]

[1] L. Que, Jr., *Nat. Struct. Biol.* **2000**, *7*, 182.
[2] E. I. Solomon, T. C. Brunold, M. I. Davis, J. N. Kemsley, S. K. Lee, N. Lehnert, F. Neese, A. J. Skulan, Y. S. Yang, J. Zhou, *Chem. Rev.* **2000**, *100*, 235.
[3] S. J. Lippard, *Nature* **2002**, *416*, 587.
[4] R. H. Holm, P. Kennepohl, E. I. Solomon, *Chem. Rev.* **1996**, *96*, 2239.
[5] D. E. Wilcox, *Chem. Rev.* **1996**, *96*, 2435.
[6] D. A. Whittington, S. J. Lippard, *J. Am. Chem. Soc.* **2001**, *123*, 827.
[7] M. I. Davis, A. M. Orville, F. Neese, J. M. Zaleski, J. D. Lipscomb, E. I. Solomon, *J. Am. Chem. Soc.* **2002**, *124*, 602.
[8] R. L. Rardin, W. B. Tolman, S. J. Lippard, *New J. Chem.* **1991**, *15*, 417.
[9] A. Lombardi, C. M. Summa, S. Geremia, L. Randaccio, V. Pavone, W. F. DeGrado, *Proc. Natl. Acad. Sci. USA* **2000**, *97*, 6298.
[10] M. Hogbom, Y. Huque, B. M. Sjoberg, P. Nordlund, *Biochemistry* **2002**, *41*, 1381.
[11] M. Merkx, D. A. Kopp, M. H. Sazinsky, J. L. Blazyk, J. Muller, S. J. Lippard, *Angew. Chem.* **2001**, *113*, 2860; *Angew. Chem. Int. Ed.* **2001**, *40*, 2782.
[12] C. F. Yocum, V. L. Pecoraro, *Curr. Opin. Chem. Biol.* **1999**, *3*, 182.
[13] V. V. Barynin, M. M. Whittaker, S. V. Antonyuk, V. S. Lamzin, P. M. Harrison, P. J. Artymiuk, J. W. Whittaker, *Structure* **2001**, *9*, 725.
[14] D. E. Ash, J. D. Cox, D. W. Christianson, *Met. Ions Biol. Syst.* **2000**, *37*, 407.
[15] L. Di Costanzo, H. Wade, S. Geremia, L. Randaccio, V. Pavone, W. F. DeGrado, A. Lombardi, *J. Am. Chem. Soc.* **2001**, *123*, 12749.
[16] M. C. Wilce, C. S. Bond, N. E. Dixon, H. C. Freeman, J. M. Guss, P. E. Lilley, J. A. Wilce, *Proc. Natl. Acad. Sci. USA* **1998**, *95*, 3472.
[17] S.-B. Yu, S. J. Lippard, I. Shweky, A. Bino, *Inorg. Chem.* **1992**, *31*, 3502.
[18] In small-molecule complexes, typical bridging bond distances are 2.18–2.25 Å in μ-H_2O–Mn^{II}_2, 2.05–2.09 Å in μ-OH–Mn^{II}_2, and 1.78–1.81 Å in μ-O–Mn^{III}_2.
[19] B. Ye, T. Mak, I. D. Williams, X. Li, *Chem. Commun.* **1997**, 1813.
[20] K. Wieghardt, *Angew. Chem.* **1989**, *101*, 1179; *Angew. Chem. Int. Ed. Engl.* **1989**, *28*, 1153.
[21] Z. Shirin, V. G. Young, Jr., A. S. Borovik, *Chem. Commun.* **1997**, 1967.
[22] J. J. Falke, G. L. Hazelbauer, *Trends Biochem. Sci.* **2001**, *26*, 257.
[23] J. J. Chou, S. Li, C. B. Klee, A. Bax, *Nat. Struct. Biol.* **2001**, *8*, 990.
[24] COLLABORATIVE COMPUTATIONAL PROJECT, NUMBER 4, *Acta Crystallogr. D* **1994**, *50*, 760.
[25] J. Navaza, *Acta Crystallogr. A* **1994**, *50*, 157.
[26] G. N. Murshudov, A. A. Vagin, E. J. Dodson, *Acta Crystallogr. D* **1997**, *53*, 240.
[27] T. A. Jones, J. Y. Zou, S. W. Cowan, M. Kjeldgaard, *Acta Crystallogr. A* **1991**, *47*, 110 *(Pt2)*.
[28] H. Sugeta, T. Miyazawa, *Biopolymers* **1967**, *5*, 673.
[29] R. M. Esnouf, *Acta Crystallogr. D* **1999**, *55*, 938 *(Pt4)*.
[30] R. A. Sayle, E. J. Milner-White, *Trends Biochem. Sci.* **1995**, *20*, 374.

  0044-8249/03/11504-0436 $ 20.00+.50/0